

ENergetic Trans-Iron Composition Explorer (ENTICE): A mission concept

1996-35

W.R. Binns, P.L. Hink, and M.H. Israel

Washington University, St. Louis, MO. 63130

T.L. Garrard, R.A. Leske, R.A. Mewaldt, and S.M. Schindler

Caltech, Pasadena, CA. 91125

L.M. Barbier, E.R. Christian, J.W. Mitchell, J.F. Ormes, R.E. Streitmatter

Goddard Space Flight Center, Greenbelt, MD 20771

M.E. Wiedenbeck

Jet Propulsion Laboratory, Pasadena, CA. 91109

C.J. Waddington

University of Minnesota, Minneapolis, MN. 55455

ABSTRACT

We describe a mission concept which has as its primary objective the measurement of the elemental abundances of galactic and solar energetic nuclei over the charge range of $14 \leq Z \leq 92$. The instruments would have sufficient collecting power to improve the number of particles collected over that of previous measurements by more than an order of magnitude and, more important, will have the capability to clearly distinguish individual elements. These measurements are of fundamental importance to an understanding of the origin, nucleosynthesis, and acceleration of energetic galactic and solar particles.

Keywords: Cosmic ray, ultra-heavy, scintillating fibers, solar energetic particles

1. Introduction and Statement of Mission Objectives

The objective of the ENergetic Trans-Iron Composition Explorer (ENTICE) is to make new measurements of unprecedented precision of the elemental composition of energetic cosmic matter with atomic number, Z , greater than 30. Precision measurements of these rare elements are of fundamental importance to an understanding of the origin, nucleosynthesis, and acceleration of energetic galactic and solar particles. Preliminary studies have suggested that these objectives could be achieved with a Midex class platform launched into an elliptical orbit. Two complementary instruments would be included, one to measure galactic and one to measure solar elemental abundances. Both instruments would have sufficient collecting power to improve the number of particles collected over that of previous measurements by more than an order of magnitude and, more important, will have the capability to clearly distinguish individual elements.

The galactic element experiment (GELEX) has been sized so that in two years sufficient nuclei can be collected to permit detailed study of the GCR elemental distribution over the full range of atomic numbers $14 \leq Z \leq 92$. In addition, based on our experience studying heavy nuclei from accelerators, we are confident of achieving the resolution required to allow unambiguous identification of individual elements, both the even- Z and the less abundant odd- Z nuclei.

The solar experiment (CUSP) would perform the first measurement of the abundances of individual SEP elements over the entire range $14 \leq Z \leq 92$. The numbers of particles expected are similar to those for GELEX, and accelerator calibrations demonstrate resolution sufficient to resolve individual elements. CUSP will provide solar abundances for many elements that are difficult to study spectroscopically, and it can also address several other key objectives for

understanding particle acceleration on the sun, in interplanetary space, and at the termination shock.

It is valuable to perform these experiments together since they provide complementary information on galactic and solar abundances that cannot be obtained in any other way. The galactic cosmic rays are believed to be a sample of matter that has been accelerated within the last ~ 10 million years. Thus they may contain a component of recently synthesized material. The solar abundances are those which existed 4.6 billion years ago when the solar system condensed out of the interstellar medium. A comparison of abundances of key elements will enable us to study galactic chemical evolution over that time period. In addition, it appears that the plasma processes that apparently fractionate the composition of the corona with respect to the photosphere also may play a similar role in the GCR composition.

2. UH Galactic Cosmic Ray Science (GELEX)

Cosmic ray nuclei with $Z > 30$ are of great interest since they include a sample of galactic matter that is believed to be synthesized in supernovae (SN). Knowledge of the elemental abundances of these nuclei can help us answer questions about their origin, the nucleosynthesis processes in which they were created, their selection and injection into the cosmic ray beam, their acceleration, their propagation to earth, their age, and the evolution of galactic matter.

Our current knowledge of ultra-heavy (UH) elemental abundances is derived primarily from the HEAO-3¹, ARIEL-6², and LDEF³ experiments. In addition, the TREK experiment has flown on MIR⁴ and analysis is in progress. The element resolution of the HEAO and ARIEL experiments was adequate to resolve peaks for the even-Z nuclei up through $Z=60$ but was insufficient to resolve any odd-Z elements, which are less abundant than their even-Z neighbors. Nuclei heavier than $Z=60$ were resolved only as groups of nuclei. The LDEF experiment is sensitive only to nuclei with $Z \geq 75$ and the MIR sensitivity falls off near $Z=55$. One of the strengths of the GELEX experiment is that it is fully sensitive over the full range of $14 \leq Z \leq 92$, thus avoiding the need for normalizing to other experiments. Those experiments which have already reported results have been valuable in the initial exploration of the UH nuclear region. However, a number of fundamental astrophysical questions about the nature of these heavy cosmic rays remain unanswered. As will be described below, the mission described here would provide valuable new information relevant to these questions.

2.1 FIP or Volatility?

One of the major discoveries that has emerged from studies of energetic cosmic matter is that essentially all samples of accelerated matter exhibit a fractionation relative to solar system abundances⁵ which is well-ordered by the first ionization potential (FIP) of the element. In general, nuclei with a high FIP are depleted relative to those with a low FIP. This has been shown to apply for solar energetic particles (SEP), solar wind (SW) nuclei, galactic cosmic ray (GCR) nuclei with $Z \leq 30$, and for those GCR elements with $Z > 30$ that have been individually measured⁶. High-FIP GCRs ($Z \leq 30$) are depleted by a factor of $\sim 5-8$ while SEPs are depleted by a factor of about 4⁷. Figs. 1a and 1b show the ratio of GCR abundances, propagated back to the source, to solar system (SS) abundances plotted versus FIP for $Z < 30$ and $Z \geq 30$ nuclei respectively. The FIP effect is evidently an atomic phenomenon which results in the preferential selection of nuclei for acceleration in the cosmic rays and, as such, might seem of modest interest. However the existence of this effect and the details of which elements are affected can provide important clues as to the origin of UH nuclei as shown below. SEPs with low FIP are believed to be preferentially selected from an ion-neutral gas in the chromosphere and photosphere where $T \sim 10^4$ K. It seems very likely that the same mechanism is operative in many other stars which eject mass, and this could be one of the primary injectors of GCR nuclei.

However, while the abundances of GCR are well ordered by FIP, it has also been shown that the abundances are well-ordered by the volatility of the elements (and their likely compounds) in an astrophysical setting^{8,9}. Volatile elements are underabundant in the GCR

relative to more refractory elements, suggesting preferential selection and acceleration of elements found in interstellar grains. Distinguishing between FIP and volatility as the ordering parameter is essential for an understanding of the origin of GCR, but it is difficult because for most elements whose primary abundances have been measured in the GCR, those that have a high-FIP are volatile and those with a low-FIP are refractory. Some of the odd-Z elements whose abundances will be measured for the first time with GELEX break this ambiguity.

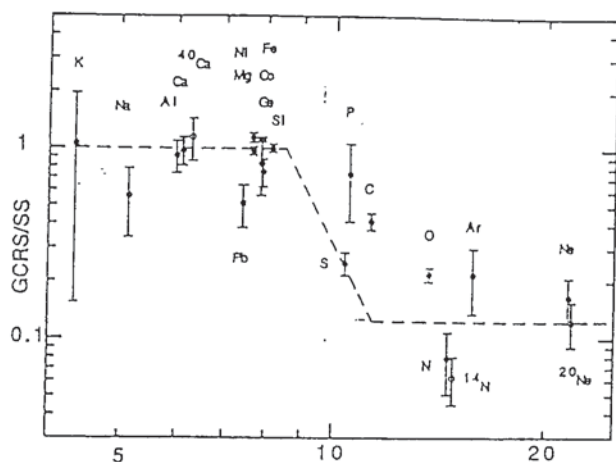


Fig. 1a--Ratio GCR source to SS abundances. Most nuclei plotted are for $Z \leq 28$ (Ferrando).

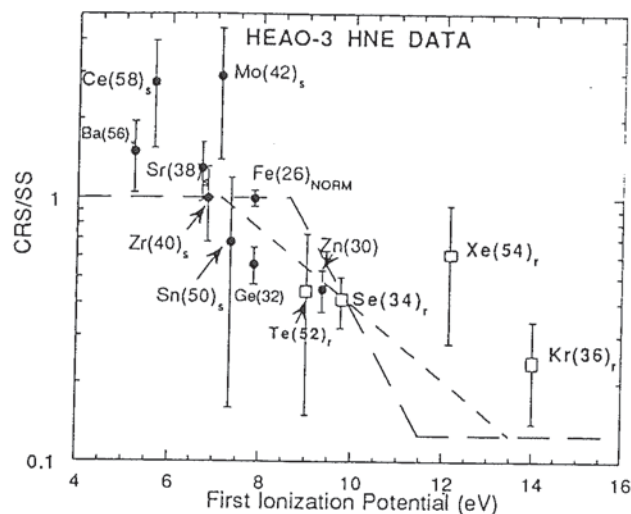


Fig. 1b--Ratio of HEAO-3 GCR source to SS abundances. R-process nuclei are shown as open squares; s-process nuclei are filled circles. The dashed lines are FIP functions derived from $Z \leq 30$ abundances

In Fig. 2 the condensation temperature is plotted vs. FIP for the UH elements¹⁰. We see that most refractory elements have a low-FIP while all of the volatile UH elements that have been measured either have a high-FIP or are well into the transition region between low- and high-FIP. We see that there are 6 elements that have been measured with high-FIP or in the transition region and that these are all volatile nuclei. Of the low-FIP nuclei which have been measured, only two are volatile while the remaining 8 are refractory nuclei.

Although all elements with a significant primary component can provide some information about the source, those with a relatively high primary fraction provide the highest sensitivity. Looking at Fig. 2, the triplet formed by the primary elements ^{34}Se , ^{37}Rb , and ^{38}Sr is of particular interest (three circles joined by dashed lines). ^{34}Se and ^{37}Rb are both r-process, volatile elements with ^{34}Se possessing a relatively high FIP and ^{37}Rb a very low FIP. They also have a high primary fraction. The ratio of these two element abundances should clearly show if FIP is important in this charge region. ^{38}Sr , on the other hand, has a low FIP as does ^{37}Rb , but is refractory. Thus the ratio of these two element abundances will indicate whether volatility is the determining factor. We note that for both of these ratios it is the presently unknown odd-Z nucleus abundance of ^{37}Rb that is the key since both ^{34}Se and ^{38}Sr have already been measured, although with relatively poor statistical precision.

A second triplet consisting of ^{52}Te , ^{55}Cs , and ^{56}Ba which is the chemical analog of the first triplet is also shown in Fig. 2. This triplet can provide similar information about the importance of FIP and again the key is the as-yet-unmeasured odd-Z element, ^{55}Cs . In the $Z \geq 60$ charge range, the existence of FIP fractionation can best be studied by comparing the abundances of some of the rare-earth nuclei with low-FIP such as ^{60}Nd , ^{62}Sm , ^{64}Gd , ^{66}Dy with the higher FIP elements ^{76}Os , ^{77}Ir , and ^{78}Pt . All of these elements are refractory and all but ^{60}Nd are r-process nuclei. Thus any depletion for the high-FIP elements should give evidence in favor of FIP fractionation, not volatility. A general enhancement of all of these elements, which HEAO and ARIEL appeared to observe, would indicate enhanced r-process nuclei over

that of the solar system. It should be noted that the highest sensitivity in discriminating between the different underlying physical processes should be obtained by fitting abundance patterns of all relevant nuclei. Measurements of those elements with presently unknown abundances in the

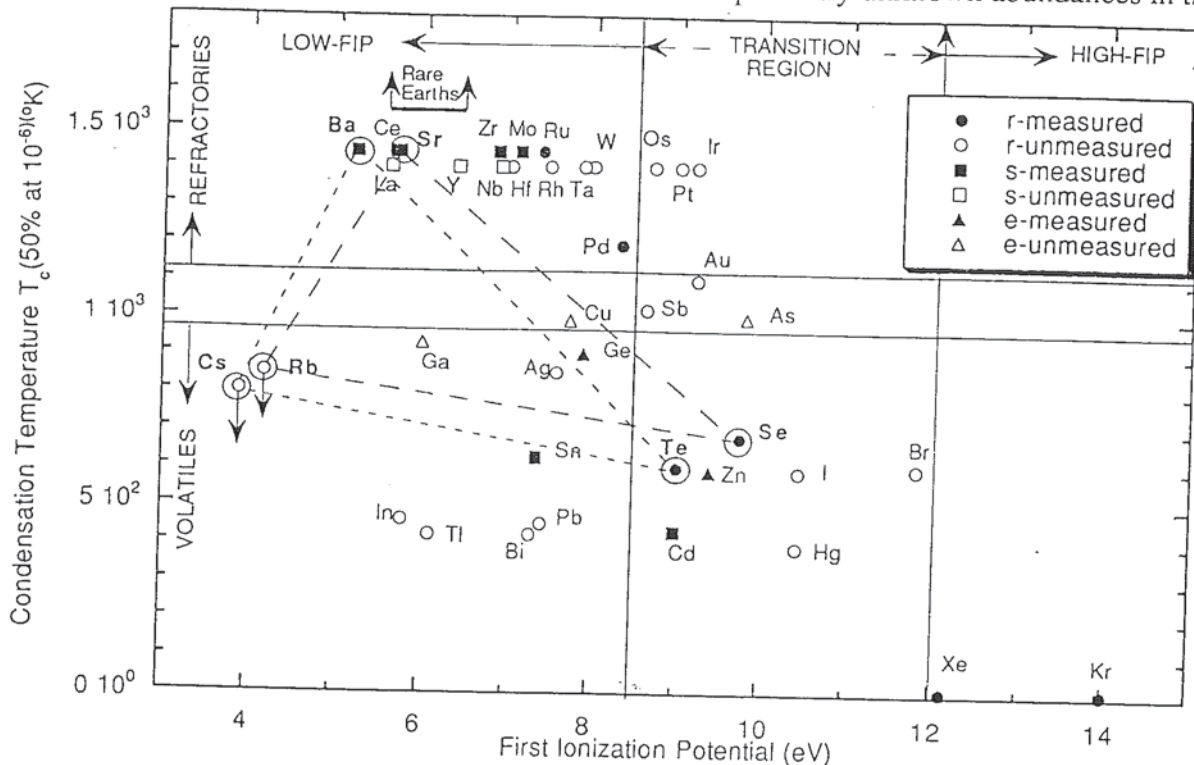


Fig. 2--The condensation temperature is plotted vs FIP for the UH elements. The circles, squares, and triangles denote elements which are primarily r, s, and e process elements respectively. The closed symbols represent those elements measured by HEAO-3. Open symbols are for elements with unknown abundances in the cosmic radiation (Figure taken, in part, from Meyer, 1981).

GCR taken together with improved measurements of those which were determined by HEAO-3 should enable us to distinguish unambiguously between sources affected by FIP or by volatility. If it is volatility then the source of GCRs would almost certainly be grains.

2.2 Do $Z < 30$ and $Z \geq 30$ Nuclei Have a Common Source?

If FIP is the organizing parameter, it is important to better determine where the transition region from normal abundances to depleted abundances occurs for UH nuclei. Fig. 1b shows two sloping step functions that have been fit to abundance data¹¹. The long dashed line is a better fit to $Z \leq 28$ abundances (Fig. 1a)⁷, but the short dashed line is a better fit to the UH data (Fig. 1b). In Fig. 2 we see that there are a number of unmeasured elements including ^{76}Os , ^{77}Ir , and ^{78}Pt that can help to better determine the transition region, if FIP is operative. If the transition from normal to depleted abundances for UH nuclei are significantly different than for $Z \leq 30$ nuclei then this would be strong evidence for separate sources.

2.3 Fresh r-Process Nuclei?

One of the important questions in cosmic ray studies has been whether a component of UH cosmic ray nuclei is accelerated in the SN in which they are synthesized. It is important to note that the r-process nuclei that have been measured with precision have a relatively high FIP and are volatile. Thus neither FIP nor volatility fractionation has been tested specifically for r-process nuclei¹². If those nuclei were freshly synthesized and accelerated in SN, they would

not be expected to exhibit either a FIP or volatility effect. Thus we see that if the element ratios show that neither FIP or volatility is operative, then this would strongly suggest "fresh" SN material. Although some current models argue against a substantial fraction being directly accelerated fresh SN material because of adiabatic losses in the expanding SN shell, we really have no experimental evidence one way or the other for r-process nuclei.

2.4 What is the age since nucleosynthesis of the heaviest UH nuclei?

Although the predicted number of Th and U that we expect to detect in two years is small (~ 10), by cleanly resolving the elements we will be able to determine whether there is more Th or U. That result in and of itself is capable of determining whether these nuclei are approximately the same age as the probable propagation time of about 10 million years or are nearer to the age of the solar system¹³. Clearly this is an objective that would benefit from an extended mission. It should be noted that the TREK-MIR experiment may have already collected approximately 10 actinides. However, their data analysis is in progress and no results are known at present.

2.5 How far away are the nearest cosmic ray sources?

Measurements of secondary GCR with $Z < 30$ indicate that the nuclei we see have experienced a distribution of path-lengths as they propagated from the acceleration sources to us. The distribution is approximately exponential, with a mean of about 7 g/cm^2 . However comparison of secondaries of C, N, and O whose interaction mean free path (mfp) in the ISM is of order 8 g/cm^2 with those of $Z=26$, whose mfp in the ISM is 3 g/cm^2 , indicate some sort of truncation of the path-length distribution at short path-lengths, below about 1 g/cm^2 . If this is established for UH nuclei, it could be interpreted as a shortage of nearby sources or the traversal of a substantial amount of matter during acceleration. The most sensitive test for nearby cosmic-ray sources will be the abundances of secondaries at the highest Z ; elements around Pt and Pb have mfp in the ISM of about 1 g/cm^2 . The cleanest measurement of secondary elements with $Z >$ comes primarily from measurements of odd- Z elements, whose abundances will be measured for the first time with this experiment.

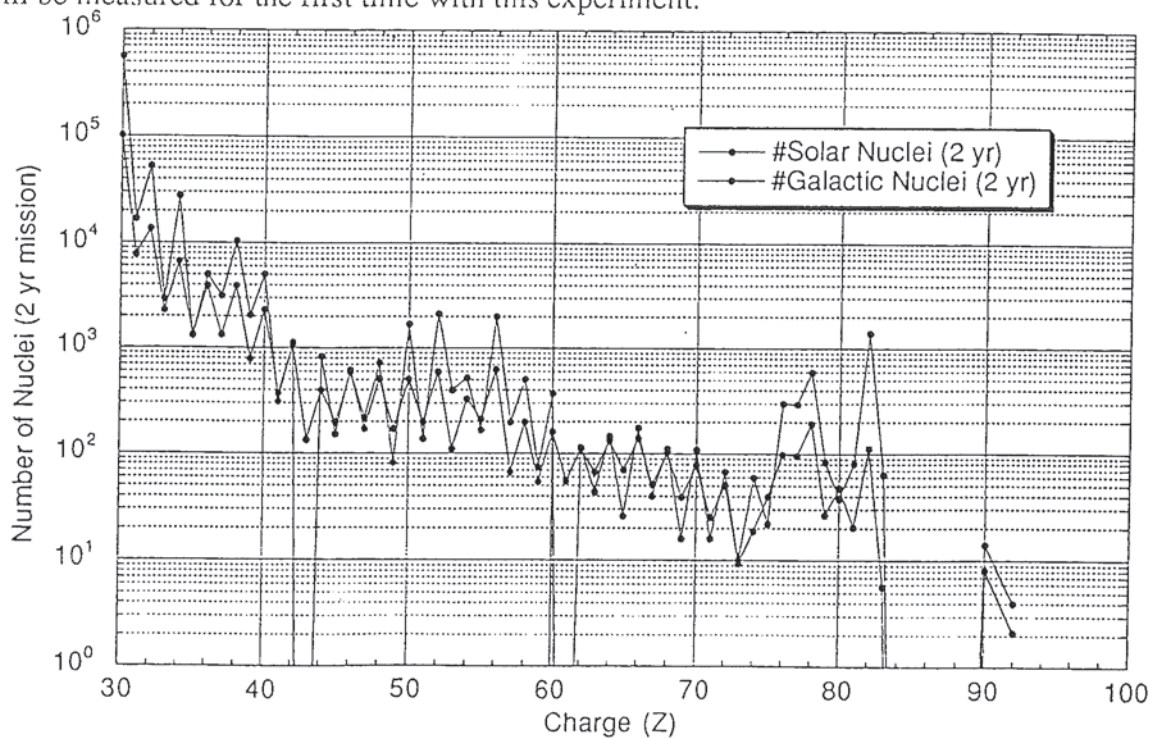


Fig. 3--The numbers of galactic and solar nuclei are estimated for a 2 year mission.

2.6 Clock nuclei?

Clock nuclei can be used to determine the time between nucleosynthesis and cosmic ray acceleration. ^{43}Tc and ^{61}Pm are interesting since their longest lived isotope beta decay half-lives are 4 million years and 2.6 years respectively. However, ^{97}Tc decays by electron capture

with half life 2.6 million years and Pm has several isotopes that decay by electron capture, with the longest half life being 5.5 years for ^{146}Pm . It is expected that even though the solar system abundances of these elements are zero owing to their decay lifetimes, those isotopes which decay only by electron capture will be present in the cosmic rays as products of interstellar interactions of heavier nuclei. The signature of a primary component would be a larger abundance than could be accounted for by interactions during propagation.

2.7 Numbers of Particles

The numbers of particles that can be collected have been calculated assuming a full geometry factor of $7 \text{ m}^2\text{sr}$ for particles entering front and back of our axially symmetrical instrument. An elliptical orbit with apogee $6R_E$ was assumed (see sect. 4) so that the earth did not significantly obstruct the viewing angle for $>80\%$ of the orbit. The numbers of particles assuming 2 years at a particle flux of $0.75 \times$ solar minimum (a reasonable average over the solar cycle) are plotted in Fig. 3 (open circles). Particles expected to interact in the detector have been excluded. These numbers correspond to 1.7×10^8 iron nuclei which compares to the much lower resolution HEAO+Ariel data set of 1.7×10^7 iron nuclei. The statistics are sufficient to achieve our goals over the full charge range. Only for nuclei with $Z \geq 60$ will the uncertainties from statistics be roughly equivalent to propagation uncertainties.

3. Ultra-Heavy Elements in Solar Material

Although the Sun contains more than 99% of the material in the solar system, most of our knowledge of the abundances of the elements in the upper two-thirds of the periodic table comes from studies of meteoritic material. Spectroscopic studies of UH elements in the solar atmosphere are made difficult by the rarity of these elements, and for many species there are no appropriate lines. In the recent summary of photospheric abundances by Anders and Grevesse⁵ there was no photospheric abundance information for $\sim 25\%$ of the elements with $Z > 30$, with relatively large uncertainties for many of the remaining elements.

Coronal shocks associated with coronal mass ejections (CMEs) and impulsive solar flares frequently inject large fluxes of energetic nuclei into the interplanetary medium. Measurements of these solar energetic particles (SEPs) can provide a direct measure of the composition of the solar atmosphere, and studies of SEPs with $Z \leq 28$ have been an important source of abundance information for many elements^{14,15}. A key discovery of SEP studies was that the coronal composition differs from that of the photosphere -- SEP-based coronal abundances of elements with FIP $> 10 \text{ eV}$ are depleted by a factor of ~ 4 ^{14,15,16}. The solar wind shows the effects of a similar fractionation, with a dependence on FIP that is much weaker in high speed streams than in slow solar wind¹⁷. Geiss and Bochsler¹⁸ have argued that the "first ionization time" (FIT) is the more relevant parameter than FIP. A goal of SEP composition measurements is to correct for these fractionation effects and deduce photospheric abundances¹⁴. The similarity between the fractionation in these solar samples and in GCRs suggests that SEPs and GCRs may have a related origin¹⁶.

With its large collecting power CUSP could extend studies of individual elements in SEPs into the upper 2/3 of the periodic table. Figure 4 shows the number of events with $>3 \text{ MeV/nuc}$ expected in two years. While SEP yields vary over the solar cycle, 8 of the 11 possible launch years should yield as many or more than Figure 4, based on scaling from measured Fe spectra¹⁹ and the solar cycle distribution of large SEP events²⁰.

3.1 Comparison of SEP and GCR Abundances:

Measurements of SEPs are important for interpreting GCR source abundances because they provide a template for comparing two samples of matter of different origin, apparently subjected to similar fractionation processes. Comparing the SEP-based coronal composition with GCR source material the FIP-related differences effectively cancel, and there is broad overall agreement, along with important differences that provide clues to the origin of GCR source material. GCRs are overabundant in C, and depleted in He, N and Ne. The overabundance of C and ^{22}Ne has been interpreted as evidence that ~25% of heavy cosmic rays originate in Wolf-Rayet stars²¹, in which case enhancements are expected in Co, Cu, and Ga ($Z = 27, 29$, and 31)²². Olive and Schramm²³ have suggested that it is the solar system that is anomalous because of nucleosynthesis inputs at the time of its formation. They predict an excess of s-process elements in GCRs.

3.2 Heavy and Ultra-heavy Ions in Impulsive Solar Flares:

It is now recognized that there are two general classes of SEP events [e.g., 15]. "Gradual" events are characterized by extended rise times and relatively long durations. They are associated with CMEs and thought to be accelerated by shocks from these events. The average abundances are typical of coronal material. "Impulsive" solar flares are generally smaller events, typically marked by enhanced fluxes of heavy nuclei (e.g., Fe), the rare isotope ^3He , and energetic electrons. Extrapolation of the apparent charge or mass dependent enhancement of Fe and other heavy elements in impulsive flares suggests that Pt-Pb nuclei may be overabundant by a factor of ~100 or more. Indeed, measurements of fossil tracks in meteoritic and lunar material find a significant overabundance of UH nuclei in SEPs [24]. The GSFC instrument on ISEE-3 (ICE) observed several hundred impulsive flares from 1978 to 1991 and Reames [25] estimated that ~1000 such events occur per year. With a geometry factor >100 times that of the ISEE-3 instrument, CUSP will be sensitive much smaller impulsive events. Extension of these studies into the UH region would provide important new information on the acceleration mechanism.

3.3 Other Objectives:

In addition to its primary objective of measuring UH nuclei in SEP events, CUSP would be able to study the composition of a variety of other energetic particle components, including anomalous cosmic rays (ACRs), a sample of the neutral interstellar material accelerated to cosmic ray energies at the termination shock. ACRs should include elements beyond the Fe-group, and other rare species, as well as the lighter elements (He, C, N, O, Ne, and Ar) that have already been discovered. CUSP would also be able to study the composition of nuclei with $Z \geq 14$ accelerated in corotating interaction regions (CIRs).

There are also interesting possibilities for CUSP to take advantage of the proposed polar orbit to use the Earth's field as a magnetic spectrometer, to study the charge states of SEP ions [26], [27], to search for SEPs that are re-accelerated to high energies at the termination shock [28], and to study recently discovered multiply-charged ACRs [29], which provide a "clock" on the acceleration rate at the termination shock.

Finally, CUSP would also be able to study the radiation belt at $L \approx 2$ composed of trapped ACRs [30] as well as other trapped heavy ions [31]. All of these studies would benefit from the fact that CUSP would have orders of magnitude more collecting power than previous instruments that have measured heavy ions from a polar orbit, such as those on SAMPEX.

4. Galactic Experiment Concept--GELEX

The GELEX instrument builds upon the strengths of the HEAO Heavy Nuclei Experiment (HNE)[1], the accelerator based Ultra-Heavy Interaction Collaboration (UHIC) [32,33], and the balloon-borne Trans-Iron Galactic Element Recorder (TIGER)[12]. The instrument complement, shown in Fig. 4, consists of Cherenkov radiation detectors (C), gas ionization

chambers (IC) operated at 1 atmosphere pressure, a scintillating fiber time-of-flight detector (TOF), and a scintillating fiber hodoscope (H). The geometrical factor is $7 \text{ m}^2\text{sr}$ for entry from either direction. The primary charge determination is obtained from the Cherenkov and ICs, as in the HEAO and UHIC instruments. Abundances derived from the HEAO data were limited to even-Z elemental abundances above $Z=28$ and elemental groups above $Z=60$ due to small scale spatial non-uniformity of knock-on electron production in the screen wire electrodes. For the UHIC experiments, the ion chambers were redesigned with smooth aluminized mylar electrodes, and when combined with a Cherenkov detector, resulted in a charge resolution of <0.15 charge units for ^{79}Au nuclei with energy 10.6 GeV/n . In Fig. 6 we show data obtained from the UHIC experiment at Brookhaven for ^{79}Au nuclei at 10.6 GeV/n and for ^{57}La nuclei at 0.62 GeV/n . The IC's relativistic rise can be used to measure energy up to at least 1 TeV/n , as demonstrated by HNE [34]. A degeneracy in the IC vs. C charge determination resulting from relativistic rise in the ICs, is resolved in GELEX by the velocity measurement of the TOF counter. The TOF measurement, including traversal direction, will be used to calibrate the Cherenkov and IC detectors' areal response. Charge estimates using both TOF-C and TOF-IC

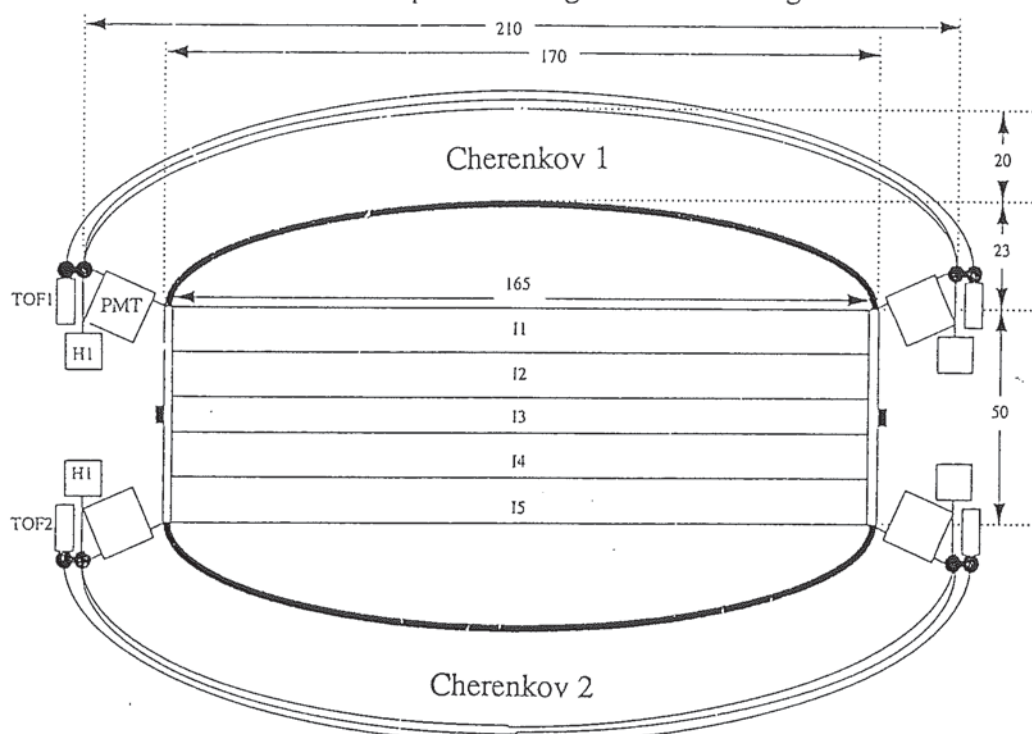


Fig. 4: Cross-sectional view of GELEX (Dimensions in cm).

validate the C-IC charge measurement for each event.

The fiber TOF consists of two layers of scintillating fibers separated by at least 100 cm . Each layer is made of 8 paddles composed of multiple layers of scintillating fibers having a total thickness of 3 mm . Both ends of the paddles are read out by fast PMTs. Based on results from the TIGER experiment [12], the expected timing resolution is 35 ps for relativistic Fe (Fig. 5 shows the timing resolution obtained for 155 MeV/n Ar, O, and C nuclei). The particle's velocity is determined to better than $0.01c$.

The fiber hodoscope is configured as three layers of 0.5 mm square cross-section fibers crossed at 60 degrees on top and bottom. Fibers from each layer are formatted onto two 3 inch crossed-anode PMTs such that the position uncertainty is $<0.2 \text{ cm}$.

The Cherenkov counters consist of an 0.8 cm thick roughened plastic radiator (Pilot 425 equivalent) in a light diffusion box, viewed by 32 five-inch PMTs. The estimated light yield is



16 p.e./minimum ionizing particle. Each PMT is individually pulse height analyzed. Each of the five ionization chambers, housed in a sealed pressure vessel containing 1 atmosphere of Ar or Kr plus CH₄, consists of two 5 cm gaps on either side of a common anode. The electrodes are made of aluminized mylar stretched on stainless steel rings, similar to the UHIC design.

Processing of phototube and IC signals will be done with custom VLSI circuitry originally designed by CIT for use on the Advanced Composition Explorer (ACE). The time-of-flight readout will be based on low power electronics being developed by GSFC for the ISOMAX

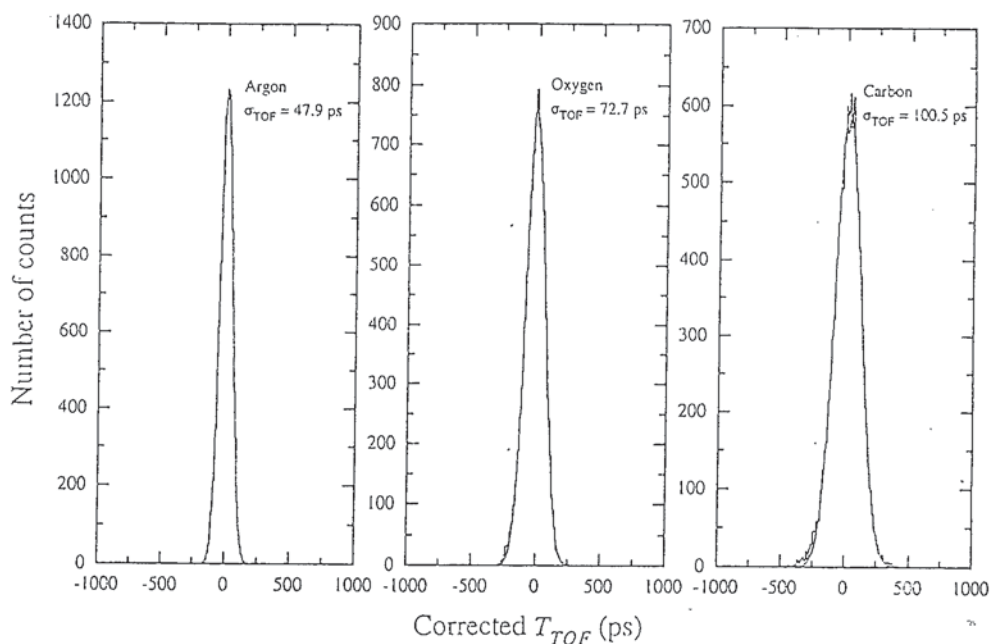


Fig. 5--Resolution in time-of-flight measurement obtained with two scintillating fiber planes for 155 MeV/n Ar nuclei.

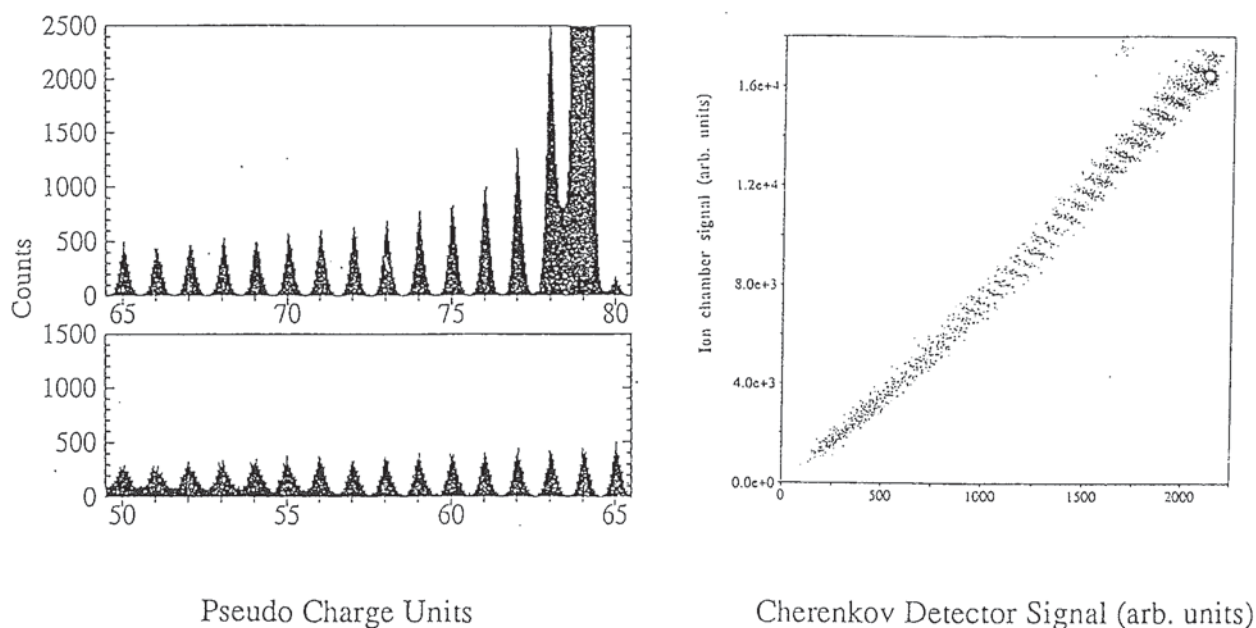


Fig. 6--Charge response of UHIC experiment for a) 10.6 GeV/n Au and b) 0.62 GeV/n La. The charge is determined from ionization and Cherenkov measurements.

experiment. The fiber hodoscope readout will be accomplished using multianode PMTs with resistively divided x-wire, y-wire position and individual wire discriminators. A calibrated pulsed laser coupled to a fiber-optic light distribution system will provide calibration pulses for timing and relative PMT gain. The event processor will acquire pulse height, TDC, and discriminator data for each event. Pulse height corrections for pathlength and position will be made prior to final acceptance of each event. PGAs will be utilized throughout the design to minimize power and complexity. Each event will contain 3264 bits of raw data. On-board data processing reduces this to 1080 bits per event, or 3600 bps at a rate of 3.3 events per second, assuming that only 1/10th of $Z \leq 26$ events with $E < 2 \text{ GeV/n}$ are telemetered.

5. Solar Experiment Concept--CUSP

Fig. 7 is a schematic illustration of an instrument capable of measuring the composition of solar energetic particles up through the platinum-lead region ($Z \sim 80$) of the periodic table. Particle identification is based on measurements of dE/dx vs. total energy for nuclei which stop in the active volume of a gas ionization chamber operated at a pressure of nominally ~ 0.2 to 0.5 atmospheres. A uniform electric field is maintained throughout this volume by an array of appropriately biased electrodes that surround it. An energetic charged particle leaves a track of electrons and positive ions in its wake. The electrons drift with a velocity of $\sim 4 \text{ cm/ms}$ to the detector's anode where they produce the electrical signals needed to identify the particle's total energy, rate of energy loss, and trajectory.

The anode is segmented into a series of conductors for sampling the particle's track. In addition to providing the needed energy loss measurements, pairs of wedge-shaped electrodes yield track coordinates in the direction parallel to the anode. Coordinates in the drift direction are derived from the particle drift time by analysis of the digitized anode signal waveforms.

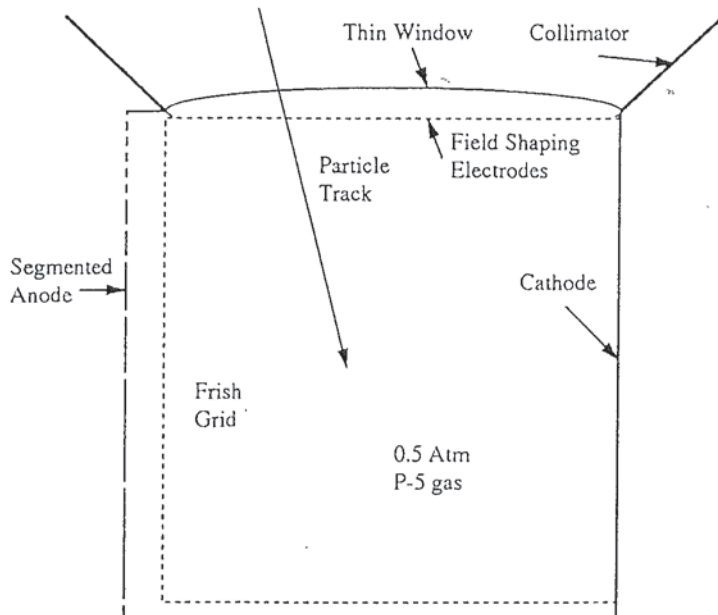


Fig. 7-CUSP Instrument Concept

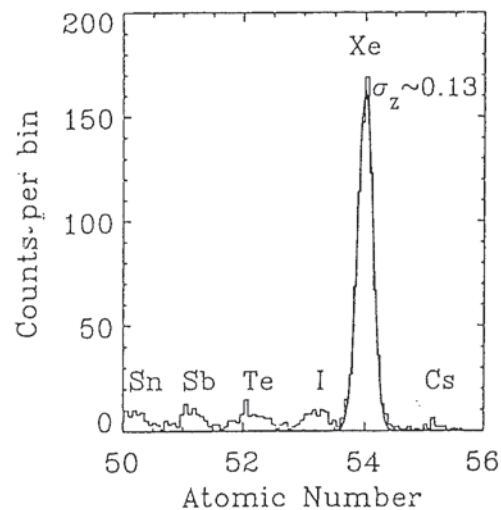


Fig. 8--CUSP resolution at accelerator

In order to obtain statistically significant samples of the rarest ultraheavy elements from the SEP events, the design strives to minimize the energy threshold to take advantage of the steep energy spectra characteristic of SEP events. The threshold energy is $\sim 3 \text{ MeV/nuc}$ for all elements with $Z \geq 26$. The depth of the active volume sets a maximum energy of $\sim 20 \text{ MeV/nuc}$ for particles which stop in the gas. This maximum can be extended by including a set of silicon solid state detectors in the back of the active volume.

The instrument design illustrated in Fig. 7 has an average geometrical factor of $\sim 1000 \text{ cm}^2 \text{sr}$ restricting consideration to particles with angles of incidence less than 45° . Data from 2 years

with typical solar maximum SEP activity will allow abundance determinations for most UH elements with accuracies of $\leq 10\%$.

To study the UH composition in large SEP events requires high-resolution measurements in the presence of intense fluxes of light particles. In a typical large SEP event (e.g., 13 Feb 1978), the time-averaged integral flux of protons plus alpha particles above 1 MeV/nuc was $\sim 10^4/\text{cm}^2\cdot\text{sr}\cdot\text{sec}$. This corresponds to $>10^7$ particles/sec in the proposed instrument. By virtue of this high rate and the small pulse heights (characteristically a percent or less of the pulse heights expected from the UH particles of interest) protons and alpha particles contribute a DC signals current of ~ 0.1 mA plus small fluctuations. Signals from the UH nuclei of interest stand out prominently above this baseline. For heavier nuclei, rates are significantly lower and pulse heights are larger: the integral fluxes for all $Z \geq 6$ elements with $E > 1$ MeV/nuc in the same flare amount to $\sim 20/\text{cm}^2\cdot\text{sr}\cdot\text{sec}$.

In order to extract the UH signals of interest from the background of lighter particles, the proposed instrument's electronics would digitize the signal waveform using "time slices" approximately 100 ns long. This significantly reduces the area (or, equivalently, time) over which the signal from a UH particle is susceptible to pile-up with a lighter nucleus. It also allows clear identification of, and to some extent, correction for instances of pileup. With appropriate fitting, one can also use the digitized waveform to derive the particle's drift time with an accuracy of ~ 25 ns, sufficient for the trajectory measurement.

Tests of a prototype multi-anode ionization chamber have been carried out using accelerator beams of energetic ^{54}Xe nuclei. Fig. 8 shows an example of the charge resolution achieved. As part of these tests, some Xe data were collected in the presence of a high background rate of light particles. Although the analysis of these data is not yet complete, preliminary indications are that excellent charge resolution is still achieved for Xe nuclei. Previous tests of gas ionization detectors showed that for elements up through the iron group it may be possible to identify individual isotopes.

6. Mission Characteristics

The preliminary mission concept calls for a two-year, midex class mission. Total mass to orbit

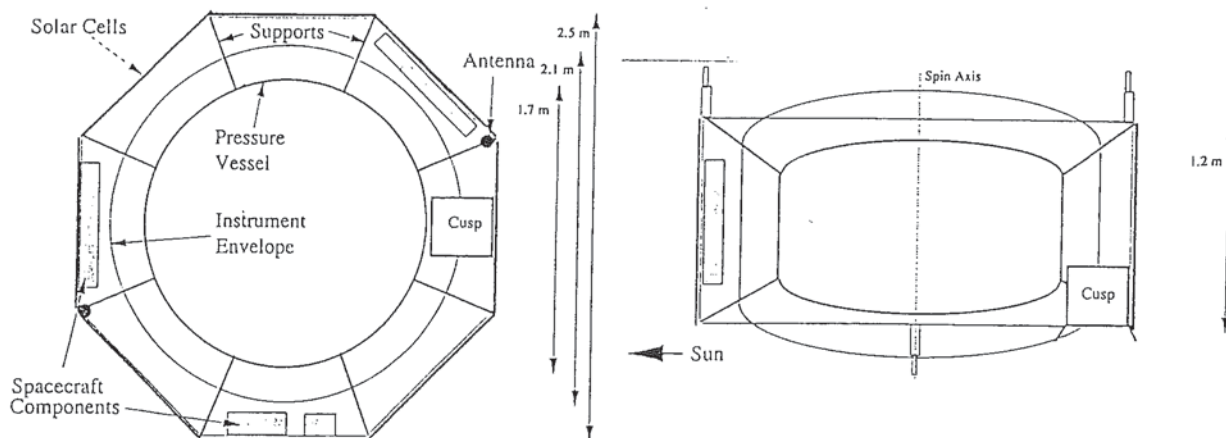


Fig. 9: Cross sections of ENTICE with instruments mounted in spacecraft.

is projected to be 760 kg for the baseline concept. The preliminary orbit is a 90° inclination, elliptical orbit with $\geq 6R_E$ apogee and a perigee sufficient to provide ≥ 2 yr lifetime. This orbit yields a high flux of both solar and galactic energetic particles and minimizes the dose from the radiation belts. The GELEX structure will serve as the main spacecraft structure, with the spacecraft components attaching directly to it. CUSP will attach directly to GELEX with its

field of view oriented approximately perpendicular to the spin axis (Fig. 9). The spacecraft will be spin stabilized about the z-axis, thus minimizing requirements on the attitude control system.

References

1. Binns, W.R., T.L. Garrard, P.S. Gibner, M.H. Israel, M.P. Kertzman, J. Klarmann, B.J. Newport, E.C. Stone, and C.J. Waddington, *Ap. J.*, **346** (1989) 997.
2. Fowler, P.H., R.N.F. Walker, M.R.W. Masheder, R.T. Moses, A. Worley, and A.M. Gay, ARIEL 6 Measurements of the Fluxes of Ultraheavy Cosmic Rays, *Ap. J.*, **314** (1987) 739.
3. O'Sullivan, D., et al., *Adv. Space Res.*, **15** (1995) (1) 15.
4. Westphal, A.J., *Advances in Space Res.*, **15** (1995) p. (6)14. Also Westphal, AJ, and P.B. Price, Proc. of 24th ICRC (Rome) 2 (1995) 581.
5. Anders, E. and N. Grevesse, *Geochim. et Cosmochim. Acta*, **53** (1989) 197.
6. Meyer, J.P., *Adv. Space Res.*, **13** (1993) 377.
7. Ferrando, P., Cosmic Ray Propagation and Origin, in *Proceedings of the XXIII International Cosmic Ray Conference*, (Calgary, 1994) ed. D.A. Leahy, R.B. Hicks, and D. Venkatesan (1994) 279.
8. Bibring, J.P. and C.J. Cezarsky, 17th ICRC (Paris) 2 (1981) 289.
9. Sakurai, K. *Adv. Space Res.* **15** (1995) (1)35.
10. Meyer, J.P., 17th ICRC 2 (1981) 281.
11. Binns, W.R., D.J. Fixsen, T.L. Garrard, M.H. Israel, J. Klarmann, E.C. Stone, and C.J. Waddington, *Adv. Space Res.*, **4** (1984) 25.
12. Binns, W.R., *Adv. Space Res.*, **15** (1995) p. (6)29.
13. Blake, J.B., and D.N. Schramm, *Astrophys. and Space Science*, **30** (1974) 275.
14. Stone, E. C., in AIP Conference Proceedings, Vol. 183, Cosmic Abundances of Matter, ed. C. J. Waddington, (New York), p. 72, 1989.
15. Reames, D. V., *Adv. Space Research* **13**, 331, 1993.
16. Meyer, J. P., *Ap. J. Supp.* **57**, 151, 1985.
17. Geiss, J., G. Gloeckler, and R. von Steiger, *Phil. Trans. R. Soc. Lond. A.* **349**, 213, 1994.
18. Geiss J., and Bochsler, P., in *The Sun and Heliosphere in Three Dimensions*, ed. R. G. Marsden (Dordrecht, Reidel), p. 173, 1986.
19. Price, P. B., I. D. Hutchen, R. Cowsik and D. J. Barber, *Phys. Rev. Lett.* **26**, 916, 1971.
20. Feynman, J., T. P. Armstrong, L. Dao-Gibner, and S. Silverman, *J. Spacecraft* **27**, 403, 1990.
21. Casse, M., and J. A. Paul, *Ap. J.* **258**, 860, 1982.
22. Prantzos, N., et al., Proc. 19th ICRC 3, 167, 1985.
23. Olive, K. A., and D. N. Schramm, *Ap. J.*, **257**, 276, 1982.
24. Goswami, J. N., D. Lal, and J. D. Macdougall, in Proc. Conf. Ancient Sun, R. O. Pepin, J. A. Eddy, and R. B. Merrill, eds, (Pergamon, New York) p. 347, 1980.
25. Reames, D. V., in Particle Acceleration in Cosmic Plasmas Workshop, Newark, DE, 1991.
26. Leske, R. A., et al., *Ap. J.* **452**, L149, 1995.
27. Mason, G. M., J. E. Mazur, M. D. Looper, and R. A. Mewaldt, *Ap. J.* **452**, 901, 1995.
28. Mewaldt, R. A., Proc. 25th Internat. Cosmic Ray Conf (Rome) **4**, 804, 1995.
29. Mewaldt, R. A., et al., "Evidence for Multiply-Charged Anomalous Cosmic Rays", *Ap. J. Letters*, in press, 1996.
30. Selesnick, R. S., et al., *J. Geophys. Res.* **100**, 9503, 1995.
31. Kleis, T. et al., Proc. 24th Internat. Cosmic Ray Conf. **4**, 481, 1995; Jonathal, D. et al. Proc. 23rd Internat. Cosmic Ray Conf. **3**, 445, 1993.
32. Waddington, C.J., W.R. Binns, J.R. Cummings, R.L. Garrard, B.W. Gauld, L.Y. Geer, J. Klarmann, and B.S. Nilsen, *Nuc. Phys. A* **566** (1994) 427.
33. Waddington, C.J., W.R. Binns, J.R. Cummings, T.L. Garrard, L.Y. Geer, J. Klarmann, and B.S. Nilsen, *Adv. Space Res.*, **15** (1995) p. (6)39.
34. Binns, W.R., T.L. Garrard, M.H. Israel, M.D. Jones, M.P. Kamionkowski, J. Klarmann, E.C. Stone, and C.J. Waddington, *Ap. J.*, **324** (1988) 1106.